HIGHLIGHT OF THE MONTH

Ab-initio calculation of Giant Magnetoresistance in magnetic multilayers

Peter Zahn,[1] Ingrid Mertig,[1] Manuel Richter,[2] and Helmut Eschrig[2]

Technische Universität Dresden
[1]Institut für Theoretische Physik
[2]MPG-Arbeitsgruppe "Elektronensysteme"
D-01062 Dresden, Germany

Introduction

Since the discovery of giant magnetoresistance (GMR) in magnetic multilayer systems (like Fe/Cr or Co/Cu) [1, 2] several experimental and theoretical studies have been carried out to elucidate the microscopic origin of the phenomenon. Here, *ab initio* calculations of the electronic structure and of the electron scattering are of great interest.

The GMR effect occurs when successive ferromagnetic layers exhibit anti-parallel magnetization. The application of an external magnetic field brings the magnetization of the ferromagnetic layers into alignment and causes a decrease of resistivity (Fig. 1) for both current-in-plane (CIP) and current-perpendicular-to-plane (CPP) geometries (see Fig. 2).

Most theories [4, 12, 10, 9, 22, 11] try to explain the GMR by spin-dependent scattering at interfaces or bulk defects but neglect the electronic structure of the multilayer system. Attempts to include the electronic structure have been made by several authors [16, 3, 21,

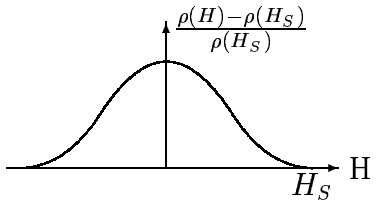

Figure 1: Giant magnetoresistance. The resistivity is maximum when the magnetic moments of successive ferromagnetic layers are antiparallel. It drops off as the applied field aligns the magnetic moments H_S, denoted by the right and left diagrams for positive and negative fields, respectively.

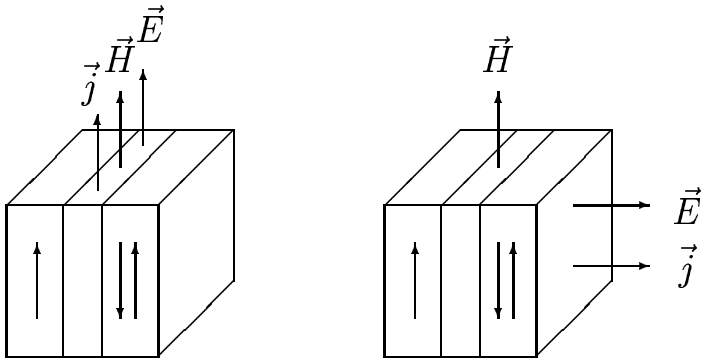

Figure 2: Geometrical arrangements of current density **j**, electrical field **E** and magnetic field **H** in CIP and CPP measurement of GMR.

23]. All calculations predict a strong influence of the electronic structure of the multilayer on the GMR.

The GMR in magnetic multilayers is defined as

$$\mathrm{GMR} = \frac{\sigma^P}{\sigma^{AP}} - 1, \tag{1}$$

where σ^P and σ^{AP} are the conductivities of the multilayer for parallel and anti-parallel alignment of successive ferromagnetic layer magnetization, respectively. Experimentally, one can be sure that parallel alignment is achieved, in view of the marked transition from strong to weak magnetic field dependence of the conductivity at the saturation field (see Fig. 1).

Electronic structure of the multilayer

Our considerations focus on (100) oriented Fe_mCr_n layer sequences (m monolayers of Fe followed by n monolayers of Cr), where the Fe layers are intrinsically ferromagnetic and the Cr layers are intrinsically antiferromagnetic. *Ab initio* electronic structure calculations have been performed using spin-density functional theory for initially parallel and antiparallel spin configurations of subsequent Fe layers [23].

Starting from the bandstructure E_k^σ of the situation, that we have just addressed, potential scattering causes transitions from a state k into a state k' of the multilayer system. The scattering can be caused by impurity atoms in the ferromagnetic or in the nonmagnetic spacer layer. The scattering is described by spin-dependent relaxation times τ^σ which are different for majority and minority electrons depending on the type of scatterer. The spin anisotropy ratio $\beta = \tau^\uparrow/\tau^\downarrow$ is a direct measure. $\beta < 1$ means strong scattering of the majority electrons and for $\beta > 1$ the minority electrons are strongly scattered.

Transport theory

Transport is described within the quasiclassical theory solving the Boltzmann equation in relaxation time approximation. Consequently, the conductivity tensor becomes

$$\hat{\sigma}^\sigma = e^2 \tau^\sigma \sum_k \delta(E_k^\sigma - E_F)\, \mathbf{v}_k^\sigma\, \mathbf{v}_k^\sigma. \tag{2}$$

The integration is performed over the Fermi surface of the parallel configuration of the layered system. Summation of the two currents yields the total conductivity

$$\hat{\sigma}^P = \hat{\sigma}^\uparrow + \hat{\sigma}^\downarrow. \tag{3}$$

In the anti-parallel configuration the electronic states are spin degenerate, and the conductivity becomes

$$\hat{\sigma}^{AP} = 2\, e^2 \tau^{AP} \sum_k \delta(E_k^{AP} - E_F)\, \mathbf{v}_k^{AP}\, \mathbf{v}_k^{AP}. \tag{4}$$

Assuming that the layered system is grown in the z direction, CIP corresponds to the xx or yy component of the conductivity tensor and CPP to the zz component in Eqs. 2 and 4. τ^{AP}, the relaxation time in the anti-parallel configuration, can be obtained by summation of the scattering operators. For equal concentration of defects in adjacent ferromagnetic layers, the relaxation time is then given by

$$\frac{1}{\tau^{AP}} = \frac{1}{2}\,\left(\,\frac{1}{\tau^\uparrow} + \frac{1}{\tau^\downarrow}\,\right). \tag{5}$$

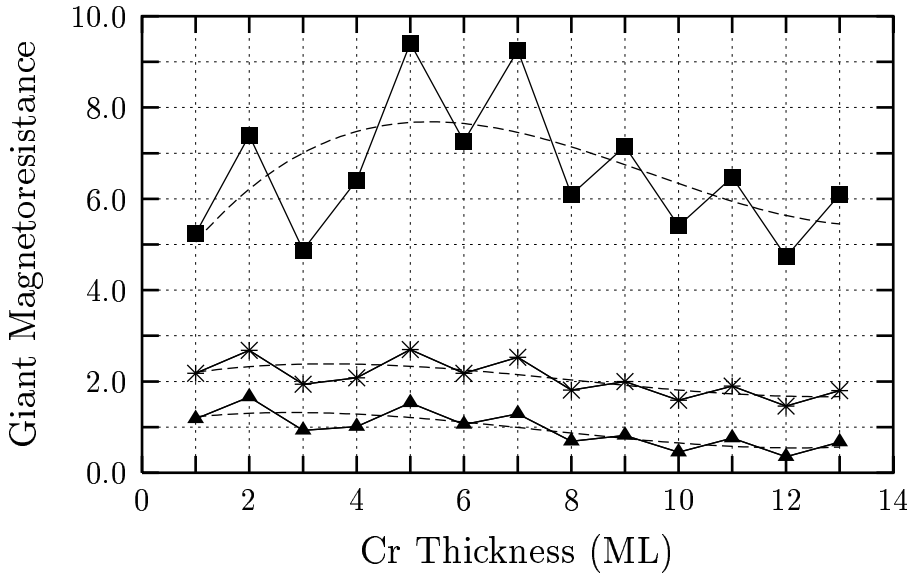

Figure 3: Calculated CIP-GMR for Fe_3Cr_n versus Cr layer thickness $n = 1, 13$. The results assuming Cr defects in the Fe layers are indicated by squares ($\beta = 0.11$). Stars mark the results for spin-independent relaxation times $\beta = 1$ and triangles for $\beta = \beta_{min}$.

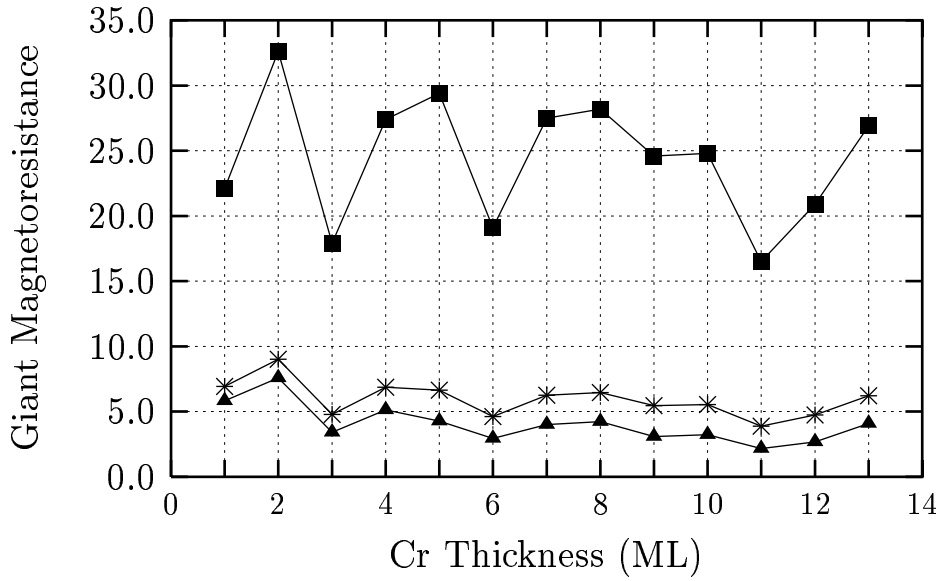

Figure 4: Calculated CPP-GMR for Fe_3Cr_n versus Cr layer thickness $n = 1, 13$. The results assuming Cr defects in the Fe layers are indicated by squares ($\beta = 0.11$). Stars mark the results for spin-independent relaxation times $\beta = 1$ and triangles for $\beta = \beta_{min}$.

Results

The simplest situation occurs, when all the scattering centers are localized in the antiferromagnetic Cr layers (for example Fe impurities).

In this case the lifetimes τ^σ for both spin directions must be equal since the spin up wavefunction amplitudes of one half of the Cr atoms is equal to the spin down wavefunction amplitudes of the other half. This corresponds to $\beta = 1$. Eq. 5 now implies $\tau^{AP} = \tau^\uparrow = \tau^\downarrow$. Hence the lifetime completely disappears from the GMR expression

$$\mathrm{GMR} = \frac{\sum_\sigma \sum_k \delta(E_k^\sigma - E_F)\, v_{k\,\mu}^\sigma\, v_{k\,\mu}^\sigma}{2\ \sum_k \delta(E_k^{AP} - E_F) v_{k\mu}^{AP}\, v_{k\mu}^{AP}} - 1. \tag{6}$$

Here, the GMR is fully determined by the Fermi surface and Fermi velocities as functions of the magnetization configuration. Hence it is a pure bandstructure effect. The obtained GMR values are about 200% in CIP and 700% in CPP (stars in Fig. 3 and 4), which is in agreement with the experimentally obtained maximum CIP-GMR (220%) for ultrathin Fe layers [20].

Simplifying Eq. 6 for further discussion of the origin of GMR leads to

$$GMR = \frac{\sum_\sigma N^\sigma(E_F) v_\mu^{\sigma\,2}}{N_{AP}(E_F)\ \ v_\mu^{AP2}} - 1 \tag{7}$$

with the density of states of the superlattice for parallel alignment

$$N_P(E_F) = \sum_\sigma\ N^\sigma(E_F) = \sum_\sigma \sum_k \delta(E_k^\sigma - E_F) \tag{8}$$

and for anti-parallel alignment

$$N_{AP}(E_F) = 2\ \sum_k \delta(E_k - E_F). \tag{9}$$

v_μ^σ and v_μ^{AP} are Fermi surface averages of the Cartesian components of the velocity for parallel

$$v_\mu^\sigma\ = \sqrt{\frac{\sum_k \delta(E_k^\sigma - E_F)\, v_{k_\mu}^{\sigma\ 2}}{\sum_k \delta(E_k^\sigma - E_F)}} \tag{10}$$

and anti-parallel alignment

$$v_\mu^{AP}\ = \sqrt{\frac{\sum_k \delta(E_k^{AP} - E_F)\, v_{k_\mu}^{AP2}}{\sum_k \delta(E_k^{AP} - E_F)}}. \tag{11}$$

The densities of states in the parallel and anti-parallel configuration (Fig. 5) are of the same order and they oscillate in phase with the Cr layer thickness, that is, they do not account for the 200% CIP-GMR and 700% in CPP-GMR (Fig. 3 and 4). Obviously, GMR is originated by the differences in the Fermi velocities in the parallel and anti-parallel configurations (Fig. 6).

The spin dependence of the relaxation time ($\beta \neq 1$) due to scattering centers in the ferromagnetic layers (Cr impurities in Fe layers, for example) leads to modifications.

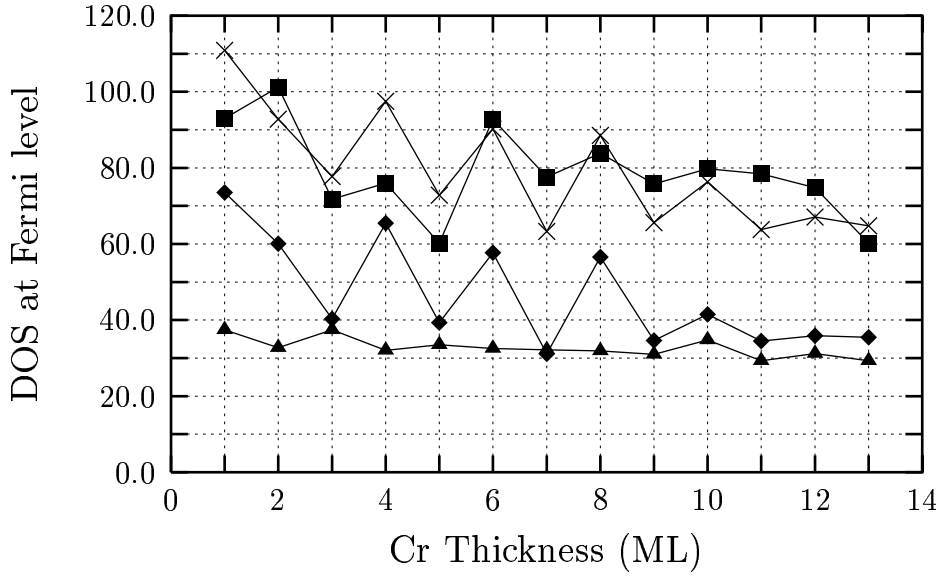

Figure 5: $N_P(E_F)$ (squares) and $N_{AP}(E_F)$ (times) of Fe_3Cr_n superlattices versus Cr layer thickness in arbitrary units. The spin-projected densities of states of $N_P(E_F)$ are marked as follows: $N^{\uparrow}(E_F)$ (diamonds) and $N^{\downarrow}(E_F)$ (triangles) [13].

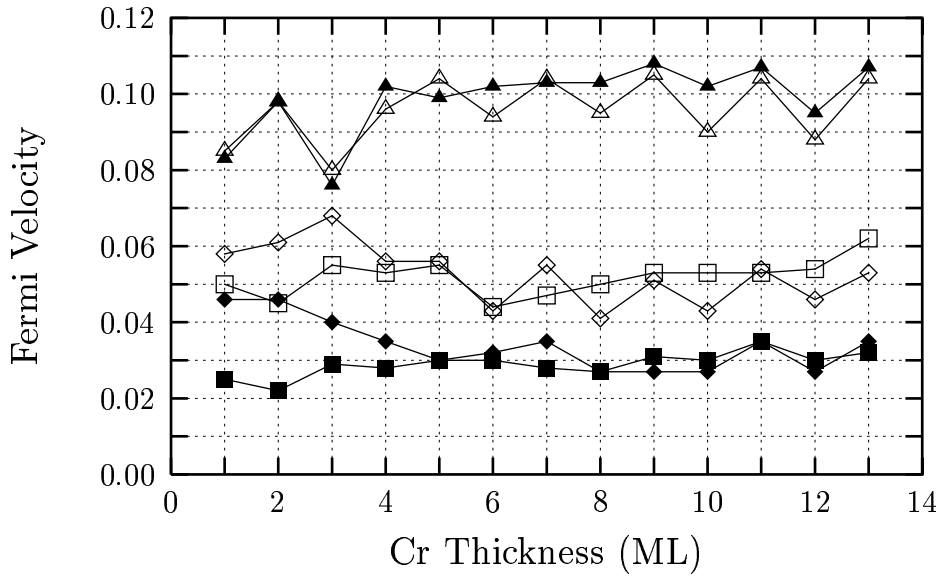

Figure 6: Fermi surface averages of the velocity components. Open symbols indicate v_x and full symbols v_z. Diamonds mark the velocity of majority electrons, triangles the velocity of minority electrons and squares the velocity in the anti-parallel aligned configuration [13].

GMR is now to be calculated via Eq. 1, 2 and 4. Under the assumption that the extension of the impurity is small compared to the layer thickness, the scattering properties are described by the spin-dependent relaxation times calculated for the Cr impurities in Fe [14, 15]. For this case $\beta = 0.11$, that is, the majority electrons are scattered strongly at a Cr defect and the minority electrons are just weakly scattered as they pass the defect.

The results assuming Cr defects located in the Fe layers lead to a GMR of about 600% in CIP (squares in Fig. 3) and 2500% in CPP (squares in Fig. 4) which is larger than the experimental results [8, 6, 18, 7]. The anisotropy β obtained in [14, 15] for a variety of defects scatter from 0.1 to 10. Therefore, GMR is discussed as a function of β in relaxation time approximation. If only one type of scatterer is included, GMR becomes a minimum for

$$\beta_{min} \;=\; \frac{\tau^{\uparrow}}{\tau^{\downarrow}} = \sqrt{\frac{\sum_k \delta(E_k^{\downarrow} - E_F)\; v_{k\mu}^{\downarrow\,2}}{\sum_k \delta(E_k^{\uparrow} - E_F)\; v_{k\mu}^{\uparrow\,2}}}. \tag{12}$$

That is, GMR can be enhanced or reduced by spin-dependent impurity scattering. The results for $\beta = \beta_{min}$ are shown in Fig. 3 and 4 (triangles).

Finally, we discuss the combination of alternating Fe layers with Cr defects ($\beta = 0.11$) and with Cu defects ($\beta = 3.68$). For the sake of simplicity, equal concentration is assumed. The relaxation times are in parallel configuration

$$\frac{1}{\tau^{\sigma}} = \frac{1}{2}\,\Big(\,\frac{1}{\tau_{Cr}^{\sigma}} \;+\; \frac{1}{\tau_{Cu}^{\sigma}}\,\Big), \tag{13}$$

and in anti-parallel configuration

$$\frac{D_{\uparrow}^{+} + D_{\uparrow}^{-}}{\tau^{\uparrow}} = \Big(\,\frac{D_{\uparrow}^{+}}{\tau_{Cr}^{+}} \;+\; \frac{D_{\uparrow}^{-}}{\tau_{Cu}^{-}}\,\Big), \tag{14}$$

and

$$\frac{D_{\downarrow}^{+} + D_{\downarrow}^{-}}{\tau^{\downarrow}} = \Big(\,\frac{D_{\downarrow}^{-}}{\tau_{Cr}^{-}} \;+\; \frac{D_{\downarrow}^{+}}{\tau_{Cu}^{+}}\,\Big), \tag{15}$$

respectively where the superscripts $+, -$ correspond to majority and minority electrons. D_{σ}^{+} and D_{σ}^{-} is the local spin-dependent density of states in a ferromagnetic layer where spin-σ electrons are majority or minority electrons, respectively. In the considered configuration the factors have been set to unity. The conductivity in the anti-parallel state including both defects is given by

$$\hat{\sigma}^{AP} = e^2(\tau^{\uparrow} + \tau^{\downarrow}) \sum_k \delta(E_k^{AP} - E_F)\; \mathbf{v}_k^{AP}\, \mathbf{v}_k^{AP}. \tag{16}$$

The results are shown in Fig. 7. The main message from this calculation is that the GMR can be reduced drastically or even change sign, if scatterers with different spin anisotropy are combined. (If they would be located in the same layer they would merely

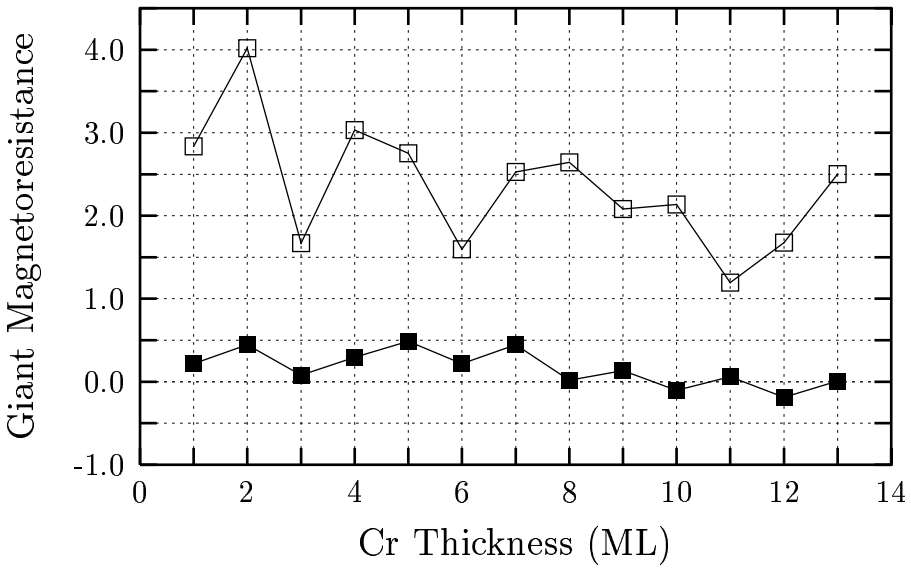

Figure 7: Calculated GMR for Fe_3Cr_n with Cr and Cu defects in adjacent Fe layers in CIP (closed squares) and CPP (open squares). For $n \geq 10$ the inverse GMR is obtained.

act as an effective scattering potential.) One should note that in Fig. 7 the inverse effect occurs in CIP but not in CPP. Experimentally, the inverse effect was obtained for $Fe/Cr/Fe/Cu/Fe/Cu$ multilayers [5], as well as in $Fe_{1-x}V_x/Au/Co$ multilayers [19], both in CIP geometry.

Generally, it should be noted that CPP-GMR for comparable scattering is always larger than CIP by a factor of about 4 in agreement with experimental results [7]. This factor stems from the difference of the Fermi velocity components in plane and perpendicular to the plane, and it finds its natural explanation in the fact that the carriers with large momentum components in direction of the current are more influenced by the superstructure in CPP.

Moreover, GMR (Fig. 3, 4, 7) shows characteristic variations with layer thicknesses. On Fig. 7 these variations are reminiscent of experimentally found oscillations [17].

Summary

In conclusion, we have shown that GMR, under the assumption of a coherent multilayer system and a spin-independent impurity scattering, is determined by the changes of the electronic structure as a function of the magnetization direction. Spin-dependent impurity scattering can enhance or reduce the effect. The combination of impurities with different spin anisotropy can in particular cause the inverse GMR.

Acknowledgement

The authors would like to thank P. H. Dederichs and R. Zeller for valuable discussions.

References

[1] M. N. Baibich, J. M. Broto, A. Fert, F. Nguyen van Dau, F. Petroff, P. Etienne, G. Creuzet, A. Friederich, and J. Chazelas, Phys. Rev. Lett. **61**, 2472 (1988).

[2] G. Binash, P. Grünberg, F. Saurenbach, and W. Zinn, Phy. Rev. B **39**, 4828 (1989).

[3] W. H. Butler, J. M. MacLaren, and X.-G. Zhang, Mat. Res. Soc. Proc. **313**, 59 (1993).

[4] R. E. Camley and J. Barnaś, Phys. Rev. Lett. **63**, 664 (1989).

[5] J. M. George, L. G. Pereira, A. Barthelemy, F. Petroff, L. Steren, J. L. Duvail, and A. Fert, Phys. Rev. Lett. **72**, 408 (1994).

[6] M. A. M. Gijs, S. K. Lenczowski, and J. B. Giesbers, Phys. Rev. Lett. **70**, 3343 (1993).

[7] M. A. M. Gijs, S. K. J. Lenczowski, J. B. Giesbers, R. J. M. van de Veerdonk, M. T. Johnson, R. M. Jungblut, A. Reinders, and R. M. J. van Gansewinkel (unpublished).

[8] M. A. M. Gijs and M. Okada, Phy. Rev. B **46**, 2908 (1992).

[9] R. Q. Hood and L. M. Falicov, Phy. Rev. B **46**, 8287 (1992).

[10] J. Inoue, A. Oguri, and S. Maekawa, J. Phys. Soc. Jpn. **60**, 376 (1991).

[11] P. M. Levy, Sol. Stat. Phys. **47**, 367 (1994).

[12] P. M. Levy, S. Zhang, and A. Fert, Phys. Rev. Lett. **65**, 1643 (1990).

[13] I. Mertig, P. Zahn, M. Richter, H. Eschrig, R. Zeller, and P. H. Dederichs, J. Mag. Mag. Mat. (accepted) (1995).

[14] I. Mertig, R. Zeller, and P. H. Dederichs, Phy. Rev. B **47**, 16178 (1993).

[15] I. Mertig, R. Zeller, and P. H. Dederichs, in *Metallic Alloys: Experimental and Theoretical Perspectives*, (Kluwer Academic Publishers, Dodrecht, Boston, London, 1994), p. 423.

[16] T. Oguchi, J. Mag. Mag. Mat. **126**, 519 (1993).

[17] S. N. Okuno and K. Inomata, Phys. Rev. Lett. **72**, 1553 (1994).

[18] W. P. Pratt Jr., S. F. Lee, J. M. Slaughter, R. Loloee, P. A. Schroeder, and J. Bass, Phys. Rev. Lett. **66**, 3060 (1991).

[19] J.-P. Renard, P. Bruno, R. Megy, B. Bartenlian, P. Beauvillain, C. Chappert, C. Dupas, E. Kolb, M. Mulloy, P. Veillet, and E. Veu, preprint (1995).

[20] R. Schad, C. D. Potter, P. Beliën, G. Verbanck, V. V. Moshchalkov, and Y. Bruynseraede, Appl. Phys. Lett. **64**, 3500 (1994).

[21] K. M. Schep, P. J. Kelly, and G. E. W. Bauer, Phys. Rev. Lett. **74**, 586 (1995).

[22] T. Valet and A. Fert, Phy. Rev. B **48**, 7099 (1993).

[23] P. Zahn, I. Mertig, M. Richter, and H. Eschrig, Phys. Rev. Lett. **75**, 2996 (1995).